



ELSEVIER

Journal of Nuclear Materials 307–311 (2002) 1–9

Journal of  
nuclear  
materials

www.elsevier.com/locate/jnucmat

## Section 1. Plenary Lectures

# ITER status, design and material objectives

R. Aymar\* and International Team

*ITER Garching Joint Work Site, Boltzmannstrasse 2, D-85748 Garching, Germany*

### Abstract

During the ITER Engineering Design Activities (EDA), completed in July 2001, the Joint Central Team and Home Teams developed a robust design of ITER, summarised in this paper, with parameters which fully meet the required scientific and technological objectives, construction costs and safety requirements, with appropriate margins. The design is backed by R&D to qualify the technology, including materials R&D. Materials for ITER components have been selected largely because of their availability and well-established manufacturing technologies, taking account of the low fluence experienced during neutron irradiation, and the experimental nature of the device. Nevertheless, for specific needs relevant to a future fusion reactor, improved materials, in particular for magnet structures, in-vessel components, and joints between the different materials needed for plasma facing components, have been successfully developed. Now, with the technical readiness to decide on ITER construction, negotiations, supported by coordinated technical activities of an international team and teams from participant countries, are underway on joint construction of ITER with a view to the signature/ratification of an agreement in 2003.

© 2002 Published by Elsevier Science B.V.

### 1. Introduction

The objective of ITER is to demonstrate the scientific and technical feasibility of fusion energy for peaceful purposes [1]. This means that ITER would demonstrate moderate plasma power amplification of  $Q \geq 10$  during an inductive burn of  $\geq 300$  s, and aim at demonstrating steady state operation with  $Q \geq 5$  as an ultimate goal, with an average 14 MeV neutron wall load  $\geq 0.5$  MW/m<sup>2</sup> and average lifetime fluence of  $\geq 0.3$  MWA/m<sup>2</sup>. Such a device would be able to demonstrate technologies essential to a reactor in an integrated system, and perform testing of high-heat-flux and nuclear components, thus satisfying the goal of a single device answering, in an integrated way, all feasibility issues needed to define satisfactorily a subsequent demonstration fusion power plant (DEMO). All the original ITER parties (Euratom, Japan, Russian Federation and the United States of America) endorsed this strategy [2], although the USA left the project in 1999. The result, documented in the ITER Fi-

nal Design Report [3] in July 2001, is a detailed, complete, and fully integrated engineering design of ITER and all technical data necessary for future decisions on its construction. This result has been achieved over the nine years of the EDA at the cost (1989 values) of \$660M (US: \$110M) on R&D, and 1950 (US: 350) professional person years of effort.

### 2. ITER design features

The major parameters of ITER are shown in Table 1. This device is optimised for its performance under inductive operation, and is appropriately equipped for steady state operation, even though the requirements for such operation are much more poorly known at this stage.

A cross section of the ITER tokamak is shown in Fig. 1. The superconducting toroidal field (TF) magnet consists of 18 coils containing circular conductor, composed of Nb<sub>3</sub>Sn strands, embedded in grooved radial plates. The central solenoid (CS) has six modules which can be powered separately. The six poloidal field (PF) coils are made using NbTi conductor in double

\* Tel.: +49-89 3299 4134; fax: +49-89 3299 4444.

E-mail address: [aymarr@itereu.de](mailto:aymarr@itereu.de) (R. Aymar).

Table 1  
Major plasma parameters and dimensions

Total fusion power (MW)	500 (700)
Q – fusion power/additional power	$\geq 10$
Average neutron wall load (MW/m <sup>2</sup> )	0.57 (0.8)
Nominal inductive burn time (s)	400
Major radius (m)	6.2
Minor radius (m)	2.0
Current (MA)	15 (17) <sup>a</sup>
Elongation (separatrix)	1.85
Triangularity (separatrix)	0.49
Safety factor (95% flux surface)	3.0
Toroidal field @ 6.2 m radius (T)	5.3
Plasma volume (m <sup>3</sup> )	837
Plasma surface (m <sup>2</sup> )	678
Heating/current drive power (MW)	73 <sup>b</sup>

<sup>a</sup> Attainment of this current, with the other parameters shown in parentheses places some limitations over other parameters (e.g. pulse length).

<sup>b</sup> Total plasma heating power up to 110 MW may be installed in subsequent operation phases.

pancakes. These latter coils are designed with redundant turns and a margin in current to avoid the need to replace the coils in case of local damage in one of the coil pancakes. To accommodate field errors due to manufacturing inaccuracies or to misalignments during assembly of the magnet coils, as well as to control resistive wall mode plasma instabilities, superconducting saddle-shaped correction coils are placed around the machine outside the TF magnets.

The reaction chamber consists of a vacuum vessel supporting exchangeable modular in-vessel components. The vacuum vessel consists of nine toroidal sectors, joined by field welds. The vessel is a double-walled stainless steel welded ribbed shell, with internal shield plates and ferromagnetic inserts to reduce TF ripple. The 421 blanket modules have a single-curvature faceted separate first wall attached to a shielding block which is remotely attached to the vessel through 3 cm diameter access holes in the first wall. To accommodate differential thermal expansion and electromagnetic loads, these attachments are stiff radially, but flexible transversely. The plasma-facing components are beryllium armour attached to a copper heat sink, mounted on a stainless steel support. The outboard modules may later be replaced with tritium breeding modules. The 54 cassette single null divertor has carbon targets and tungsten high heat flux components, again mounted on a copper heat sink and stainless steel structure bolted to rails on the vessel floor. The targets can accommodate heat loads of more than 20 MW/m<sup>2</sup> for 20 s, but the more normal peak heat load will be between 5 and 10 MW/m<sup>2</sup>.

Seven of the 18 equatorial ports of the vessel are used for heating antennae and neutral beam ducts, three are used for DEMO-relevant test blankets, two for plasma

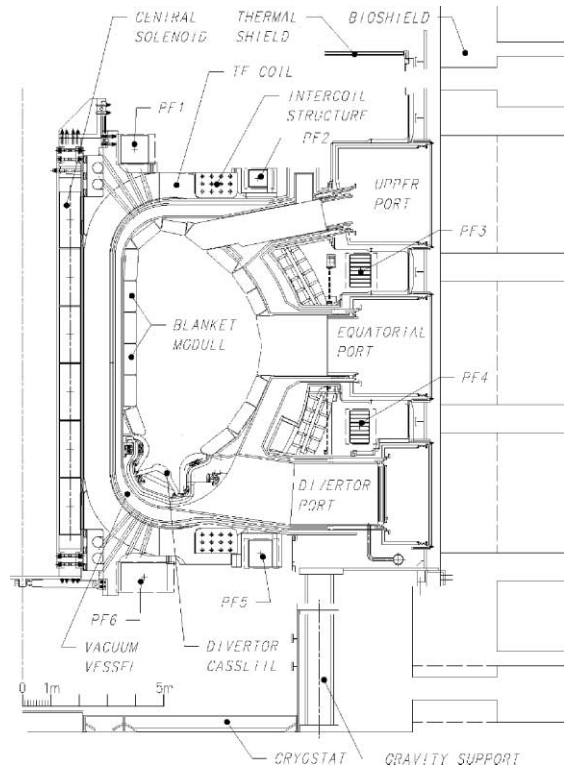


Fig. 1. ITER tokamak cross-section.

limiters, and the remainder (partly) for plasma diagnostics. The limiter and two diagnostic ports are also used for remote replacement of the blanket modules. Divertor ports accommodate up to nine torus cryopumps, diagnostics, glow discharge cleaning system, pellet and gas injection, and an in-vessel viewing system. Three divertor ports are also used for the remote replacement of the divertor cassettes, which are inserted radially and then slid toroidally and clamped to rails. The upper ports are mainly used for diagnostics and gas injection. Three contain electron cyclotron antennas to control plasma instabilities (neo-classical tearing modes).

The cryostat is essentially a reinforced single shell cylinder 24 m high and 28 m diameter with flat ends. The thickness of shielding in the machine and bioshield is arranged to permit suitably shielded personnel access at the port terminations or, exceptionally, for repairs in the cryostat-coil interspace, after shutdown.

The tokamak is water-cooled by separate and redundant circuits feeding the blanket (three circuits in parallel), divertor and limiter (one circuit), and vacuum vessel (two circuits in parallel). An additional safety feature is that the vessel cooling circuit can remove, by natural convection, all decay heat produced after shutdown by all vessel and in-vessel components. Typical

water inlet temperature is 100 °C, and pressures are in the range of 3–4.2 MPa. Baking of in-vessel components to remove impurities is carried out at 240 °C (200 °C for vessel).

The plasma is heated (and current may be driven) by a combination of electron cyclotron, ion cyclotron, lower hybrid and 1 MeV negative-ion-accelerated neutral beam systems. The initial setup will involve two neutral beams and electron and ion cyclotron systems, but the radio-frequency systems are designed in exchangeable modular fashion (20 MW/port) to allow various mixes to be tried, and three neutral beams can be accommodated on the machine. A heating power in excess of 110 MW is thus attainable.

ITER is assembled inside a cylindrical ‘pit’ embedded up to the equatorial port level. After installation of the lower cryostat, PF coils and supports, 40° sectors of the vacuum vessel are combined with two TF coils and appropriate thermal shielding, and field welded to adjacent sectors in the pit. The upper coils, ports and services are connected, and the cryostat is closed by a flat lid with heavy segmented shielding. Once the machine is radioactive, localised areas at reduced air pressure around port entrances are provided during maintenance to limit contamination spread.

### 3. Materials choice and R&D

For a fusion power reactor, the main characteristics of the materials close to the plasma is that they tolerate a high fluence from 14 MeV neutrons yet produce a small amount of radioactive waste. Thus low activation materials are desirable and must surely be developed if fusion is to provide a desirable energy source. ITER, on the other hand, will typically produce damage of only 3 dpa in the austenitic stainless steel of the first wall. With judicious use of low Nb and Co grades, this will permit most radioactive waste (except, essentially, from the blanket) to be cleared for unrestricted re-use a century from the end of operation. Despite these differences, many ITER conditions are highly relevant for reactor design choices:

- for diagnostics and their materials, which on today’s experiments experience very little radiation, but which on ITER will be in areas of high dose and whose design can cause radiation streaming to deeper structures;
- for plasma-facing materials compatible with plasma purity and with heat unload, their joint to underlying heat sinks and structures, and their coolant;
- for magnet structure which, on account of its large size, needs to be strengthened by welds which introduce weak points liable to fatigue, and for superconductor with regard to its behaviour in operation.

By far the most essential material used for ITER is austenitic stainless steel. Therefore the material choice is orientated toward industrially available materials and manufacturing technologies with suitable physical and mechanical properties. The largest share belongs to a range of 316LN grades. The following sections briefly describe the selection and assessment of materials for diagnostic components, vessel and in-vessel components, and magnets. Further details can be found in recent Refs. [4–7]

Behind the choice of each material is a large body of R&D to substantiate the properties, in the main carried out in the frame of the ITER EDA’s ‘Large R&D Projects’, which focused on the manufacture of TF and CS model coils, vacuum vessel, blanket and divertor full scale prototypes, and the proof of blanket and divertor remote maintenance

#### 3.1. Diagnostic materials

The key issue for the chosen materials (Table 2) is radiation resistance. While not all material choices are yet proven, promising candidates exist for nearly all applications.

On insulating ceramics, R&D indicates that, with careful choice of material and operating temperature range, the long-term bulk radiation-induced electrical (insulator) degradation (bulk RIED), and radiation-induced conductivity (RIC), will not cause problems, except possibly for applications such as bolometer substrates, where cross-leakage may be important. Countermeasures must be taken to mitigate surface contamination and degradation.

For the different cable types with different configuration RIC, RIED, conductor resistance, dielectric breakdown strength, and radiation-induced electromotive force between sheath and centre conductor of mineral insulating (MI) cables, are the most important properties. The last could make plasma control difficult for very long pulses (>1000 s). Recent R&D is encouraging, but further tests and analytical work are required.

Windows must be vacuum tight to UHV standards and also be able to withstand a potential 0.2 MPa pressure rise during an in-vessel coolant leak. Under high-flux ionising radiation, sapphire will have some advantages over fused silica, due to its relative insensitivity to gamma radiation, despite silica’s better radio-luminescence tolerance. In the case of diamond, excellent material grades have been developed, which can be used for diagnostic windows from the GHz region to the IR/visible range.

For a large variety of optical diagnostics one would want to use fibre optic transmission near the plasma to take advantage of the limited spatial access and easy alignment of optical components. Although only a few metres of cable will be exposed to significant radiation

Table 2  
Reference diagnostic materials

Diagnostic components/sensors	Candidate materials
Ceramics (electrical insulators)	Single crystal and polycrystal alumina ( $\text{Al}_2\text{O}_3$ )
Wires/cables	MI-cables: SUS, Inconel (sheath)/ $\text{MgO}$ , $\text{Al}_2\text{O}_3$ (insulator)/Cu, Ni (centre conductor)
Windows	Fused silica/quartz KU-1 (400–1500 nm; high OH), sapphire (800–5000 nm), diamond (GHz-IR)
Optical fibres (visible region)	Pure silica (core)/F doped (clad)/Al jacket (RF:KS-4V), F doped silica (core)/F doped (clad)/Al jacket (JA F-doped)
(IR region)	Pure silica, F doped (core)/F doped (clad)/Al jacket
Mirrors/reflectors	First mirrors: metal (Cu, W, Mo, SS, Al), LIDAR single coated (Rh/V), dielectric mirrors: ( $\text{HfO}_2/\text{SiO}_2$ , $\text{TiO}_2/\text{SiO}_2$ ), LSMs: (Mo/Si, W/ $\text{B}_4\text{C}$ and W/C), X-ray crystals: (Ge, Si, $\text{SiO}_2$ , graphite)
Magnetic coils	MI cables
Bolometers	Mica substrate, Au meander

flux, radiation resistance, particularly for optical wavelengths, is an issue, and these are a function of dopants, OH-content, impurities, cladding type, manufactured drawing speed and temperature, and preform fabrication. In the IR region (low absorption and low radio-luminescence) suitable fibres already exist. With the better radiation resistance revealed by fluorine-doped optical fibres, it should be possible to use optical fibres for the visible region inside the cryostat during operation. More extensive studies are underway.

Irradiation, sputtering, evaporation, or coating of a mirror's surfaces can all change its reflectivity. R&D has found solutions where the dominant damage mechanism is erosion for mirrors mounted facing the plasma in the equatorial and the upper ports. In the shielding labyrinths e.g. of the divertor, however, deposition could dominate, and controlled experiments on present-day devices and the development of models and possible mitigating methods are still needed.

### 3.2. Vessel and in-vessel component materials

The key issue with these components is the selection of suitable material combinations for plasma facing materials, heat sink and support structure, whose properties will be adequately maintained after a cost-effective component manufacturing process mainly involving joining. The materials grades currently selected are summarised in Table 3, but in some cases their suitability after manufacture remains to be confirmed.

Different plasma facing materials are required in different locations, depending on how local conditions influence plasma purity and material erosion.

Beryllium is used for the first wall and limiter due to its low plasma contamination and radiative power losses, good oxygen gettering, and low bulk tritium inventory. The particular grade was selected for the following qualities:

Table 3  
Main materials for vacuum vessel and in-vessel components

Material	Grade	Components
Beryllium	S-65C VHP (DSHG-200)	Armour tiles for first wall and limiter
Tungsten	Pure sintered W	Armour tiles for divertor components
CFC	SEP NB 31, NIC 01 (CX 2002U, SEP NS31)	Armour tiles for divertor vertical target
Austenitic and precipitation hardened steels	316L(N)-IG	Shield modules, vacuum vessel, blanket cooling manifolds, back-up material for divertor body, thin walled tubes for first wall, in-vessel cooling pipes
	AISI 660	Fastening components for the port plugs (e.g. fixing wedges and bolts)
	SS 30467	Boronised steel for in-wall shielding plates
Ferritic steel	SS 430	Ferromagnetic insert in shadow of TF coils to reduce field ripple
Cu and Cu alloys	CuCrZr-IG	Heat sink for plasma-facing components (PFCs) and for heating systems
	CuAl25-IG	Heat sink for PFCs
Ni alloys	Inconel 718	Bolts for the flexible supports and electrical straps, blanket cooling manifold support
Ti alloy	Ti-6Al-4V	Flexible cartridges for the module support
Ceramic	$\text{Al}_2\text{O}_3$ or $\text{MgAl}_2\text{O}_4$	Electrical insulators of module attachment and limiter plates

Note: Materials used for commercial components are not included in the table; backup materials in parentheses.

- lowest BeO and metallic impurity content among the other structural grades;
- high elevated temperature ductility;
- excellent low cycling thermal fatigue performance and thermal shock resistance.

The effects of neutron-irradiation-induced low temperature embrittlement of Be are minimised by the use of small tiles in the design.

W is the choice for the divertor baffle areas where there exists a high concentration of neutral particles. W has a lower erosion rate, due to its low sputtering yield and higher sputtering threshold energy, as compared to those of Be and C. Another advantage of W is its low tritium retention. Disadvantages are that a small amount of W in the confined plasma region could lead to a very large radiative power loss from the plasma. W also will suffer from melting if it is exposed to high peak heat loads during disruptions. A wide range of pure sintered W is available from different suppliers. The W properties database is also well established. Below 500 °C W becomes brittle at the expected fluence of 0.1–0.5 dpa in the region near the heat sink, so the design uses a brush structure to reduce thermal stresses (Fig. 2).

The lower part of the divertor vertical target uses carbon fibre composite (CFC). W and Be in this area would create and lose a melt layer during disruptions. However, CFC use has to be minimised, because of chemical erosion and tritium retention, especially in co-deposited layers. Also, at the low irradiation temperatures (<300 °C) experienced by the bulk material, the thermal conductivity could be reduced a factor ~3–5 times below that of unirradiated CFC. This leads to an increase in thermal erosion under disruptions.

For Cu alloy heat sinks for these plasma-facing materials, two candidates are retained, and the appropriate

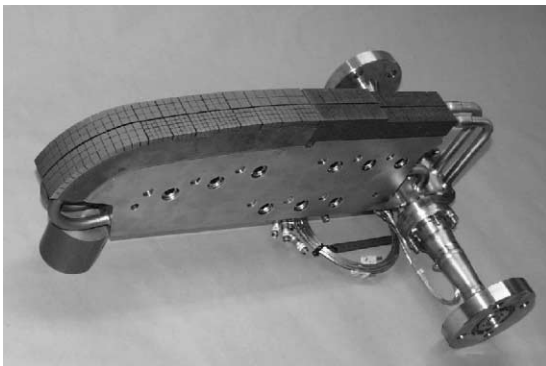


Fig. 2. Vertical target prototype (EU) produced as part of the divertor large project. Tungsten tiles are mounted on the curved part whereas carbon is used on the flat region which would receive the higher heat flux. This prototype was tested in the range 10–20 MW/m<sup>2</sup> for more than 2000 cycles.

one will be selected according to the manufacturing process, for the following reasons:

- the properties of CuCrZr alloy strongly depend on thermomechanical treatment which could be part of the manufacturing cycle, whereas properties of GlidCop® Al25 alloy are relatively independent of the heat treatment;
- fracture toughness of CuCrZr alloy is significantly higher (also after neutron irradiation) at high temperatures (>~200 °C) than that of GlidCop® Al25;
- CuCrZr is a weldable material, whereas fusion welding is not recommended for GlidCop® Al25;
- CuCrZr alloy is available from different suppliers, whereas GlidCop® Al25 is produced by one firm, OMG Americas, USA.

Thus CuCrZr would be selected, provided the manufacturing process can be arranged to minimally affect its properties, as was shown in ITER R&D (see below). Both alloys exhibit radiation hardening, decrease in ductility, and loss of work hardening capability at low neutron irradiation temperatures. Nevertheless, the performance of these materials still meet ITER requirements.

Regarding the joining of the heat sink to armour materials, many solutions were tested. For Be to Cu joints the following methods are now taken as reference:

- first wall, for GlidCop® Al25, HIP at 850 °C with a Ti interlayer – this has demonstrated satisfactory performance at a heat flux ~1–2.5 MW/m<sup>2</sup>; for CuCrZr, HIP at 500–580 °C, or fast brazing;
- high heat flux components (e.g. port limiter): ‘fast’ brazing with CuInSiNi alloy and HIP at 625 °C with AlBeMet interlayer; fast brazing demonstrated the best thermal durability, e.g. resisted 4500 cycles at 12 MW/m<sup>2</sup>.

To compensate for the large difference in the coefficient of thermal expansion and of elastic modulus, several W/Cu joining methods were developed:

- casting pure Cu onto W – the W/cast Cu elements are then joined to the Cu alloy heat sink by e-beam welding (Fig. 2), fast brazing or HIP at 480–550 °C;
- direct high temperature CuMn-alloy-based fast brazing onto CuCrZr;
- joining W rods to CuCrZr heat sinks by e.g. diffusion bonding of W rod tips directly into the OFHC/Cu-CrZr substrate.

For CFC/Cu joints there is an even larger difference in the coefficient of thermal expansion of the materials,

and increased wetting and a compliant layer is needed. The following technologies have been found to withstand the high heat fluxes:

- active metal casting (AMC<sup>®</sup>), which includes special laser treatment of the CFC surface, followed by casting of pure Cu onto CFC, machining and final joining with the Cu alloy heat sink by HIP at 480–500 °C, or e-beam welding (Fig. 2);
- direct brazing with CuMn alloy.

Type 316 L(N)-IG (ITER grade, i.e. a tighter specification of component quantities) austenitic stainless steel (SS) is the main structural material for the ITER vacuum vessel and for in-vessel components (shielding blanket, divertor cassette body). This steel is qualified in many national design codes, has adequate mechanical properties, good resistance to corrosion, has weldability, forging, and casting potential, is industrially available in different forms, and can be manufactured by well-established techniques. It has better mechanical properties than 316L and 316LN steels and is less sensitive to the radiation embrittlement of 304 steel. At welds, some ductility reduction occurs after irradiation at 275–375 °C, but this is well above ITER operating temperatures.

For SS/Cu joints, solid HIP achieves the best quality. For CuAl25-IG alloy, HIP at ~1050 °C can be used, which permits the combination in one treatment of the joining of Cu/SS and SS/SS. For CuCrZr-IG, HIP at ~920 °C is more suitable, in which case steel-to-steel joining has to be performed by a separate procedure. To maintain the good properties of CuCrZr, fast cooling is necessary and aging at 450–500 °C.

Another materials issue concerns the blanket attachments (Fig. 3). A flexible cartridge in the form of a cylinder with axial slots (Fig. 4) is screwed into the vessel from one side and bolted through access holes in the blanket. The material needs a high strength, to withstand axial loading forces and to allow for a wide range of elastic deformation during bending. Hence the choice of titanium alloy over Inconel 718 and 316 steel. This material is widely used in the chemical and aerospace industries in different countries, so the database of unirradiated material is relatively complete. Ductility is not an issue at the levels of dose that will be experienced (below 0.1 dpa), and the cartridge is shielded from the direct bombardment of energetic particles by the module itself, avoiding hydrogen implantation. ITER R&D shows that hydrogen saturation of Ti-6Al-4V alloy up to 200 wppm of hydrogen did not result in changes of tensile properties.

High strength, fatigue and fracture toughness lead to the choice of material for the bolt. The operational conditions are ~150–300 °C, ~0.5 dpa, and a fatigue life of ~30 000 full power cycles. Inconel 718 is used in the

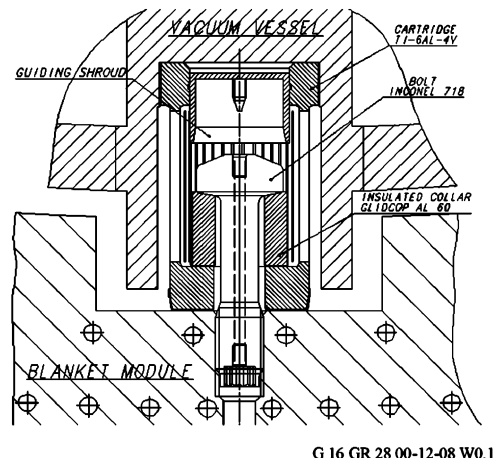


Fig. 3. Blanket flexible support attachment.



Fig. 4. Blanket flexible support cartridges (RF), developed/tested in the blanket module large project.

nuclear industry, and is produced commercially in the form of bars, rods, plates, strips, etc. Neutron irradiation up to 0.5 dpa results in an increase in strength and a slight decrease of ductility, but this does not affect the component structural integrity or lifetime. However, significant stress relaxation is expected under irradiation, and the required pre-stress should be ~800 MPa.

The blanket module insulation (alumina or spinel) plays a structural role and sustains significant static and dynamic loads. R&D over 10 000 cycles showed that plasma-sprayed coatings are not damaged if the compression stress does not exceed the yield point of the substrate material. For ITER, in the worst case, the estimated dielectric breakdown strength of these materials is almost one order of magnitude better than required. It is not expected that significant strength degradation will occur for the dose of irradiation anticipated.

### 3.3. Magnet materials

The choice of superconductor used depends on the field, temperature and current in each coil.  $\text{Nb}_3\text{Sn}$  has a higher critical temperature and field than  $\text{NbTi}$ . However it is brittle and all of the mechanical forming operations associated with the coil have to be completed before the compound is formed in the already wound conductor (Fig. 5) by a reaction heat treatment, at about  $600^\circ\text{C}$  for about 200 h, of niobium filaments distributed in a tin-bearing matrix (either bronze or copper with a central tin core). Conversely,  $\text{NbTi}$  is a metal alloy and is ductile, allowing a more conventional winding technique.  $\text{Nb}_3\text{Sn}$  and  $\text{NbTi}$  filaments show negligible effects of radiation at levels up to those corresponding to the coil insulation limits. The typical arrangement of the conductor strands and filaments is shown in Fig. 6. The strands, cooled by a flow of supercritical helium at about 4 K, are introduced into a conduit, the conductor jacket.

The material for the conductor jacket has an important structural role in the CS and PF coils, which are pulsed. For the PF coils, the jacket is fabricated as extruded sections which are assembled by butt welding. Tensile stress dominates and a refined 316LN or L austenitic steel has sufficient fatigue margin. For the CS, which is highly stressed and cycled twice per pulse from zero to full field (13 T), the material choice is much more complicated. The jacket material may have to be co-reacted through the  $\text{Nb}_3\text{Sn}$  heat treatment and both high yield strength and good fatigue resistance have to be retained. Assembly onto the brittle cable after heat

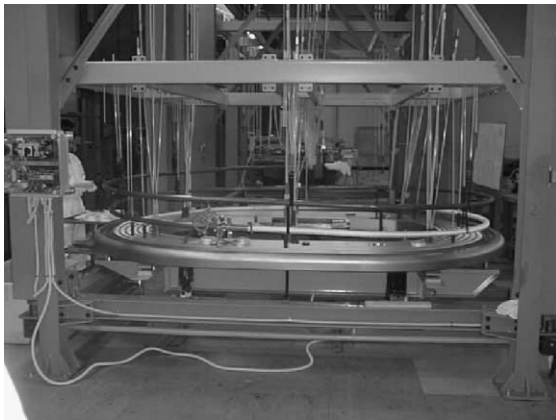


Fig. 5. Insulation process of the TF model coil conductor. After reaction to produce the  $\text{Nb}_3\text{Sn}$ , the coil pancake turns are carefully opened to allow insulation tape to be wound on. The coil using this pancake has been tested at 8 T at 80 kA (compared to 11.8 T and 68 kA in ITER), the highest superconductor current ever achieved. Testing is continuing in combination with other coils to increase the field (EU).

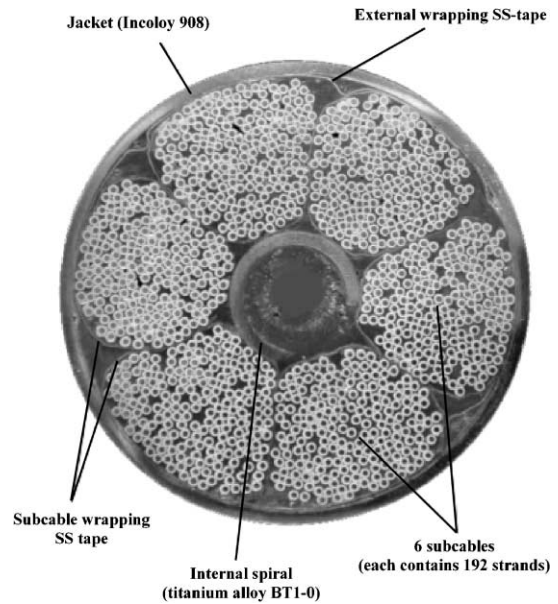


Fig. 6. Inside the CS model coil large project, the largest, high field, pulsed superconducting magnet in the world (600 MJ), a maximum field of 13 T is available to test inserts of long length ( $\sim 100$  m) built with different conductors (figure shows TF coil insert conductor).

treatment is possible, by longitudinal welding of two 316LN U-shaped halves, but requires extreme care (a thin co-reacted Ti jacket forms the conduit). It is preferable (but not an absolute requirement) for a co-reacted jacket to have a thermal contraction coefficient close to that of the  $\text{Nb}_3\text{Sn}$  strands, since the strand superconducting properties are decreased by strain. Incoloy 908 and pure titanium (with controlled oxygen content) have been specially developed for co-reaction, and have thermal contraction coefficients that match the  $\text{Nb}_3\text{Sn}$ . Incoloy 908 undergoes precipitation hardening in the reaction heat treatment, leading to a good fatigue performance, but is extremely sensitive to stress accelerated grain boundary oxidation, and this results in stringent requirements on oxygen in the heat treatment atmosphere. Modified 316LN steel has a significantly higher thermal contraction when co-reacted, and its fracture toughness is marginal.

In the CS and PF coils, made up of pancakes (or multiple pancakes) of wound superconductor, joints are necessary at each end. For some locations it is possible to join the cables by butt joint and extend the jacket containment around the whole electrical contact part. However, in some locations (the coil terminals to the busbars), this is not practical, and overlap and butt joints are used. The overlap joint needs about 500 mm to ensure uniform contact to each strand.

For the TF coils, the Nb<sub>3</sub>Sn conductor jacket has no structural role, but is merely a circular conduit built from austenitic stainless steel and co-reacted. The large mechanical loads imposed on the TF coils are reacted by the robust and thick steel coil cases built around the superconductor winding pack. These cases experience locally, at the nose and at the upper and lower inboard curved regions, very high stress levels (650–700 MPa) with a cyclic component from the interaction with the PFs. Fatigue analysis assuming initial defects ends with a requirement to be able to detect at these locations all defects large than 10 mm<sup>2</sup>.

To avoid a martensitic transition in association with fatigue crack growth, which at 4 K in 304L(N) steel can lead to fast fracture, a fully stabilised 316 class steel is required. The cost penalty of this choice is small. To achieve properties at the best end of the range covered by this steel, a class of ‘strengthened austenitic steels’ have been defined (denoted EK1, EC1, JJ1 and JK2) during ITER R&D, with specific individual compositions and suppliers. Table 4 gives a summary of materials allocated to the various components. All these materials require changes from the conventional 316LN by increasing the nitrogen content (0.2%) to increase the strength, and the manganese (above 6%) to increase the nitrogen solubility to maintain good welds.

The pre-compression ring that is used at the top and bottom of the TF coil inner leg to maintain the wedged interface of the coils under compression during cool-down and warmup is formed by winding high density glass filaments coated with epoxy binder around the circumference.

#### 4. ITER negotiations and CTA

Quadripartite meetings on negotiations on the Joint Implementation of ITER began in June 2001. The current participants are Euratom, Japan and the Russian Federation, plus Canada, which participated through Euratom in the EDA and has now made a government-backed site offer. As an original ITER party, the USA may rejoin if it wishes, and other countries may also join subject to unanimous agreement by the negotiating parties.

The tasks of the negotiators include the following:

- drafting the ITER Joint Implementation Agreement;
- selecting the ITER construction site;
- agreeing who will provide the various ITER components/systems and how the costs will be shared;
- identifying the Director General for the ITER Legal Entity (ILE) and the organisation of its work.

The negotiators are supported on technical aspects by Coordinated Technical Activities (CTA) which maintain the integrity of the project so as to prepare for joint construction and operation. A project board coordinates the activities of the ‘Participant Teams’ – one for each negotiating party – plus an International Team located at the present ITER Joint Work Sites. A ‘Standing Sub-group’ of the negotiators can call on expertise in all other relevant areas necessary to draw up the Joint Implementation Agreement.

The work of the participant and international teams during the CTA will involve preparation for an efficient start of construction, including

Table 4  
Materials for magnet structures

Specification	Components
EK1 or JJ1 forged sections	TF coil case (inner leg basic elements) including stub elements, pre-compression ring flanges
EK1 or JJ1 forged plates	Gravity support stacked plates, flanges and joint keys, friction joints webs of intermediate outer intercoil structure stub elements (fabrication option)
JK2 extruded/rolled sections	Reinforcing for Ti CS conductor jacket
JK2 forged plates	Buffer elements of CS pre-load structure (due to low thermal contraction of JK2)
EC1 cast sections	TF coil case (outer leg basic elements) including (fabrication option) outer intercoil structure stub elements
316LN forged plates	PF coils supports (frames, clamp plates, tie rods, flexible plates and bolts), parts of radial plates and covers CS supports, tie plates, flanges, adjustable wedges of CS pre-load structure
316L extruded square tubes, circular tubes and circular sections	PF coil jackets, parts of radial plates and covers VV support stacked plates and flanges, CCs supports cooling pipes
Incoloy 908 extruded square tubes	CS conductor jacket
Modified 316LN	TF conductor jacket
Titanium	CS conductor jacket
Inconel 718 as fasteners	Pre-compression ring bolts, inner intercoil structure poloidal keys and outer intercoil structure bolts joints bolts for gravity support and VV support



- design adaptations to potential sites and their regulatory environment, and formal review and modification to ensure design completeness;
- preparation of licensing applications by closer dialogue with potential host regulators;
- exploitation of physics R&D to take advantage of latest experimental results, and of manufacturing R&D;
- technical specification for procurements which need to be launched as soon as possible.

The timescale for the negotiations foresees that the government of each party interested in hosting ITER will offer a site in 2001, leading to a preferred site before the middle of 2002, and further development of design adaptations for the preferred site up to the end of the CTA at the end of 2002. The Joint Implementation Agreement should be initialled at the start of 2003 formal signature (and/or ratification) should take place in 2003.

To prepare for a site choice and its consequent sharing of contributions, the potential participants in construction must evaluate, at the highest level, the advantages and disadvantages of the various possible outcomes for their scientific institutions, industry, and strategic planning. Such preparation will significantly shorten the time taken to reach a satisfactory compromise with the other participants. If the US is interested in participating in ITER construction, it should therefore rejoin the project soon.

## 5. Conclusions

There is an undisputed need for a burning plasma experiment at the centre of fusion development. A machine integrating the appropriate physics and technology is the right next step, and ITER fulfils this role. In the materials area, for instance, ITER will confirm choices of many diagnostic, plasma-facing component, and magnet materials, and their manufacturing techniques, that will be used in future machines.

The objectives of the EDA have been fully met and the ITER design has been approved by the parties. There is consensus that it will reach its objectives. The

fusion programme is scientifically and technically ready to take the important ITER step.

Sharing costs and pooling expertise have allowed the EDA parties jointly to undertake tasks that would have been beyond their individual financial and technical capacity. The parties have developed a mature and wide-ranging capacity for successful focused international joint work. The success of the EDA demonstrates feasibility and underlines the desirability of jointly implementing ITER in a broad-based international collaborative frame: it supports the parties' declared policy to pursue the development of fusion through international collaboration. The start of negotiations on an agreement for joint construction and operation is a very positive step in their commitment to the implementation of this policy.

## Acknowledgements

This report was prepared as an account of work undertaken within the framework of ITER CTA. These are conducted by the Participants: Canada, the European Atomic Energy Community, Japan, and the Russian Federation, under the auspices of the International Atomic Energy Agency. The views and opinions expressed herein do not necessarily reflect those of the participants to the CTA, the IAEA or any agency thereof. Dissemination of the information in this paper is governed by the applicable terms of the former ITER EDA Agreement.

## References

- [1] ITER EDA Agreement and Protocol 2, ITER EDA Documentation Series No. 5, IAEA, Vienna, 1994.
- [2] ITER Special Working Group Report to the ITER Council on Task #2 Results, ITER Council Proceedings: 1999, ITER EDA Documentation Series No. 17, IAEA, Vienna, p. 33.
- [3] Technical Basis for the ITER Final Design, ITER EDA Documentation Series No. 22, IAEA, Vienna, 2001.
- [4] A. Costley et al., *Fus. Eng. Des.* 55 (2001) 31.
- [5] G. Kalinin et al., *J. Nucl. Mater.* 283–287 (2000) 10.
- [6] H. Tsuji et al., *Fus. Eng. Des.* 55 (2001) 141; N. Mitchell et al., *Fus. Eng. Des.* 55 (2001) 171.
- [7] G. Janeschitz et al., *J. Nucl. Mater.* 290–293 (2001) 1.